

GAUGING METALLICITY OF DIFFUSE GAS UNDER AN UNCERTAIN IONIZING RADIATION FIELD

HSIAO-WEN CHEN,¹ SEAN D. JOHNSON,^{2,3} FAKHRI S. ZAHEDY,^{1,4} MICHAEL RAUCH,⁴ AND JOHN S. MULCHAEY⁴

¹*Department of Astronomy & Astrophysics, The University of Chicago, 5640 S Ellis Ave., Chicago, IL 60637, USA*

²*Department of Astrophysics, Princeton University, Princeton, NJ, USA*

³*Hubble, Princeton–Carnegie fellow*

⁴*The Observatories of the Carnegie Institution for Science, 813 Santa Barbara Street, Pasadena, CA 91101, USA*

(Received May 19, 2017; Revised May 30, 2017; Accepted May 30, 2017)

ABSTRACT

Gas metallicity is a key quantity used to determine the physical conditions of gaseous clouds in a wide range of astronomical environments, including interstellar and intergalactic space. In particular, considerable effort in circumgalactic medium (CGM) studies focuses on metallicity measurements, because gas metallicity serves as a critical discriminator for whether the observed heavy ions in the CGM originate in chemically-enriched outflows or in more chemically-pristine gas accreted from the intergalactic medium. However, because the gas is ionized, a necessary first step in determining CGM metallicity is to constrain the ionization state of the gas which, in addition to gas density, depends on the ultraviolet background radiation field (UVB). While it is generally acknowledged that both the intensity and spectral slope of the UVB are uncertain, the impact of an uncertain spectral slope has not been properly addressed in the literature. This *Letter* shows that adopting a different spectral slope can result in an order of magnitude difference in the inferred CGM metallicity. Specifically, a harder UVB spectrum leads to a higher estimated gas metallicity for a given set of observed ionic column densities. Therefore, such systematic uncertainties must be folded into the error budget for metallicity estimates of ionized gas. An initial study shows that empirical diagnostics are available for discriminating between hard and soft ionizing spectra. Applying these diagnostics helps reduce the systematic uncertainties in CGM metallicity estimates.

Keywords: methods:data analysis – galaxies:halos – quasars:absorption lines – galaxies:abundances

arXiv:1706.04645v1 [astro-ph.GA] 14 Jun 2017

1. INTRODUCTION

The presence of heavy elements is expected to alter both the thermal and chemical states of a gas cloud. For example, the radiative cooling function depends sensitively on the gas metallicity. For a fixed gas density, a higher-metallicity gas is expected to cool faster under the same radiation field. In addition, formation of molecules and dust grains also depends strongly on gas metallicity. At a fixed surface gas density, a higher molecular gas fraction is seen in higher metallicity gas. Gas metallicity is therefore a key quantity that determines the physical conditions of gaseous clouds in a wide range of astronomical environments, including interstellar and intergalactic space (see Somerville & Davé 2015 for a recent review and comprehensive prior references).

It is well established that the intergalactic medium (IGM) has been enriched with heavy elements since early times (see McQuinn 2016 for a recent review). Heavy ions are also routinely observed, through absorption features imprinted in the spectrum of a background object, in the circumgalactic medium (CGM) beyond visible galaxies (e.g., Chen et al. 2010; Steidel et al. 2010; Bordoloi et al. 2011; Lovegrove & Simcoe 2011; Tumlinson et al. 2011; Borthakur et al. 2013; Stocke et al. 2013; Liang & Chen 2014; Bordoloi et al. 2014; Huang et al. 2016). The physical mechanisms that bring heavy elements to these low density regions are not well understood. Leading models include early enrichment by first galaxies (e.g., Scannapieco et al. 2002), galactic superwinds (e.g., Aguirre et al. 2001), and stripping of accreted satellite galaxies (e.g., Gunn & Gott 1972; Balogh et al. 2000). Because gas associated with starburst-driven outflows is expected to show on average higher metallicity than gas being accreted from the IGM or low-mass satellites (e.g., Shen et al. 2013), metallicity is considered a critical discriminator among these competing models and considerable effort in CGM studies focuses on metallicity measurements of the gas (e.g., Péroux et al. 2003; Kulkarni et al. 2007; Lehner et al. 2013; Werk et al. 2014; Kacprzak et al. 2014; Péroux et al. 2016; Prochaska et al. 2017).

A wide range of metallicity has been reported for the CGM at redshift $z < 1$ and projected distances of $d \lesssim 200$ kpc from galaxies, from $< 1/10$ solar to super-solar values. The large scatter implies that chemical-enrichment may be localized and mixing is inefficient. At the same time, an anti-correlation between neutral hydrogen column density ($N(\text{HI})$) and gas metallicity has also been reported over a column density range from $\log N(\text{HI}) \approx 15$ to $\log N(\text{HI}) \approx 19$ (e.g., Péroux et al. 2016; Prochaska et al. 2017). Following a declining $N(\text{HI})$ with d from previous studies (e.g., Chen et al. 1998; Rudie et al. 2012; Johnson et al. 2015), the reported anti-correlation implies a rising chemical enrichment level with increasing distances from star-forming regions. This is difficult to understand, given that heavy elements are produced in stars.

In the low-column density CGM and IGM with $\log N(\text{HI}) < 18$, gas is highly ionized. Consequently, substantial ionization corrections are necessary for inferring the total elemental

abundances from observed column densities of H^0 and various heavy ions. To determine gas metallicity, it is therefore necessary to first constrain the ionization state of the gas. In this *Letter*, we first illustrate that differences in the adopted ultraviolet background radiation field (UVB) for the ionization analysis can explain the order-of-magnitude difference in the reported CGM metallicities. We emphasize the need of including such systematic uncertainties in the error budget for metallicity estimates of ionized gas. Then we discuss results from an initial study to develop empirical diagnostics for identifying appropriate ionizing spectra for CGM absorbers, and thereby minimizing systematic uncertainties in CGM metallicity estimates.

2. THE ULTRAVIOLET BACKGROUND RADIATION FIELD

A required ingredient for photo-ionization modeling of the CGM and IGM is the ionizing radiation intensity, J_ν , which is often approximated as a power law at photon energies > 1 Rydberg (cf. Figure 1), $J_\nu = J_{912} (\nu/\nu_{912})^{-\alpha}$, with J_{912} representing the radiation intensity at 912 Å where the Lyman limit transition occurs and α representing the spectral slope. Both quasars and starburst galaxies are thought to contribute significantly to the extragalactic UVB at high redshifts (e.g., Faucher-Giguère et al. 2008). However, the redshift evolution of J_ν is highly uncertain, both in its amplitude, J_{912} , and in spectral slope, α (e.g., Haardt & Madau 2012; Kollmeier et al. 2014; Shull et al. 2015). Luminous QSOs exhibit significantly harder spectra than star-forming galaxies with a spectral slope ranging from $\alpha \approx -0.6$ to $\alpha \approx -1.8$ for QSOs (e.g., Scott et al. 2004) and $\alpha < -2$ for star-forming galaxies (e.g., Madau & Shull 1996).

The left panel of Figure 1 displays a range of model spectra, J_ν , that are commonly seen in the literature for IGM/CGM ionization studies, including (1) the Haardt & Madau 2005 (HM05) model that includes contributions from both quasars and galaxies (solid curve), (2) an HM05 quasar-only model (dotted curve), (3) the revised Haardt & Madau (2012; HM12) model (dash-dotted curve), and (4) a hybrid model that includes the default HM05 background and a local radiation field due to leakage from an L_* galaxy at 50 kpc away (red dashed curve). All Haardt & Madau models are computed using CUBA as implemented in the Cloudy software (Ferland et al. 2013, c13.05). The local radiation field is computed using Starburst99 (Leitherer et al. 1999) under the assumptions that the galaxy has been forming stars at a constant rate over the past 1 Gyr and that 2% of ionizing photons can escape. The output Starburst99 spectrum is scaled to match an intrinsic B -band magnitude of $M_{B_*} = -20.5$ expected for an L_* galaxy (e.g., Cool et al. 2012) and then combined with the default HM05 model. The purpose of including a hybrid model is to allow the possibility that a non-negligible amount of ionizing flux comes from the central galaxy of a CGM hosting halo. It is immediately clear that the primary difference between these different model spectra is in the fractional contribution of star-forming galaxies. The HM12 model assumes small escape fractions of

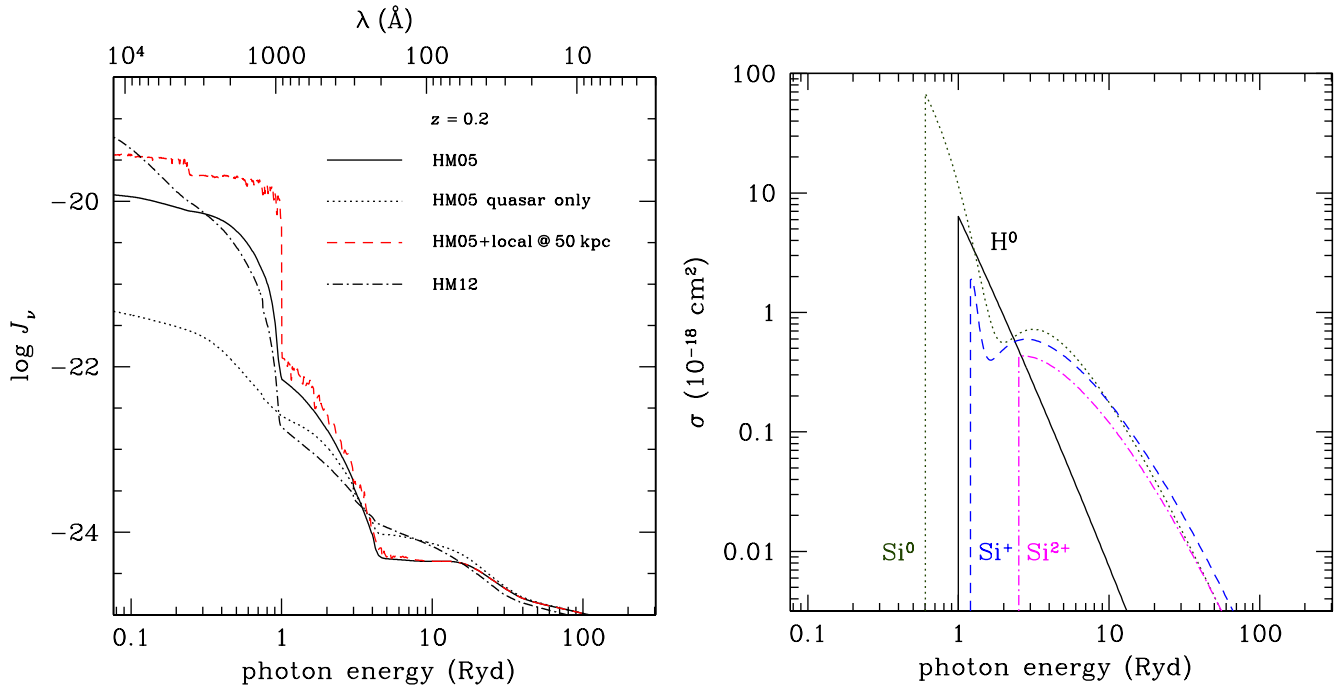


Figure 1. *Left:* Commonly adopted ionizing spectra, J_ν , for IGM/CGM ionization studies. The spectra are computed for $z = 0.2$ using *Cloudy* (version c13.05; Ferland et al. 2013) based on (1) the Haardt & Madau, HM05 model (solid curve), (2) a quasar-only model from HM05 (dotted curve), (3) the revised Haardt & Madau (2012; HM12) model (dash-dotted curve), and (4) a hybrid model that includes the default HM05 background and a local radiation field due to leakage from an L_* galaxy at 50 kpc (red dashed curve; see the main text for details). *Right:* Frequency-dependent photo-ionization cross sections of neutral hydrogen, H^0 , neutral silicon Si^0 , and silicon ions, Si^+ and Si^{2+} from Verner et al. (1996). While the photo-ionization cross section of hydrogen is sharply peaked near 1 Rydberg, the relatively flat frequency dependence of the ionization cross sections of silicon ions beyond 1 Rydberg indicate that accurate estimates of the ionization fractions of these ions depend more strongly on the accuracy of the spectral slope of J_ν at high energies. The same conclusion also applies to other heavy ions, such as C^+ , C^{2+} , C^{3+} , and Mg^+ commonly seen in the CGM.

$1.8 \times 10^{-4} (1+z)^{3.4}$ for star-forming galaxies, resulting in a diminishingly small contribution from galaxies at $z < 2$ when compared to the HM05 model. Therefore, the HM12 model resembles the HM05 quasar-only model with higher radiation intensities at energies beyond 4 Rydberg.

Empirical constraints for the UVB have relied primarily on observations of the $\text{Ly}\alpha$ forest, either from the observed mean opacity over a cosmological volume or from the observed relative deficit of $\text{Ly}\alpha$ absorption lines due to a local enhancement of ionizing radiation in the vicinities of QSOs (see Becker et al. 2015 for a review). For a photo-ionized gas, the mean $\text{Ly}\alpha$ opacity is directly related to the hydrogen photo-ionization rate, $\Gamma_{\text{HI}} = \int_{\nu_{912}}^{\infty} 4\pi [J_\nu/h\nu] \sigma_\nu(\text{H}^0) d\nu$ (e.g., Osterbrock & Ferland 2006), where $\sigma_\nu(\text{H}^0)$ is the frequency-dependent photo-ionization cross section of hydrogen. A unique advantage of observing the $\text{Ly}\alpha$ forest is that it provides a representative measure of the underlying UVB without being subject to incompleteness corrections that affect emission surveys of galaxies and quasars. However, caveats remain.

First, the conversion from the observed mean $\text{Ly}\alpha$ opacity to hydrogen photo-ionization rate relies on the knowledge of the thermal state of the IGM, which is uncertain. Uncertainties in the IGM thermal history have contributed to the large

scatters seen in the derived Γ_{HI} , which range from a factor of two at $z > 2$ (e.g., Becker et al. 2015) to a factor of six at lower redshifts (see e.g., Shull et al. 2015). Furthermore, as shown in the right panel of Figure 1, $\sigma_\nu(\text{H}^0)$ declines rapidly with increasing photon energy, following $\sigma(\text{H}^0) \propto \nu^{-3}$. Consequently, Γ_{HI} is expected to be most sensitive to the ionizing radiation intensity near the Lyman limit, J_{912} , but insensitive to intensities at higher energies (and therefore the intrinsic spectral slope α), leaving α poorly constrained.

The lack of constraints on α , particularly over 1 and 4 Rydberg, directly impacts our ability to obtain accurate measurements of gas metallicity. In the right panel of Figure 1, we also include the frequency-dependent photo-ionization cross sections of silicon in neutral, and singly- and twice-ionized states. The curves are computed based on the fitting functions provided in Verner et al. (1996). In contrast to H^0 , the mean photo-ionization rates of Si^+ and Si^{2+} are driven by high-energy photons at $\gtrsim 2$ Rydberg, making the predicted ionization fractions of these species more susceptible to uncertainties in the spectral slope (α) of J_ν .

3. GAS METALLICITY BASED ON OBSERVED IONIC ABUNDANCES

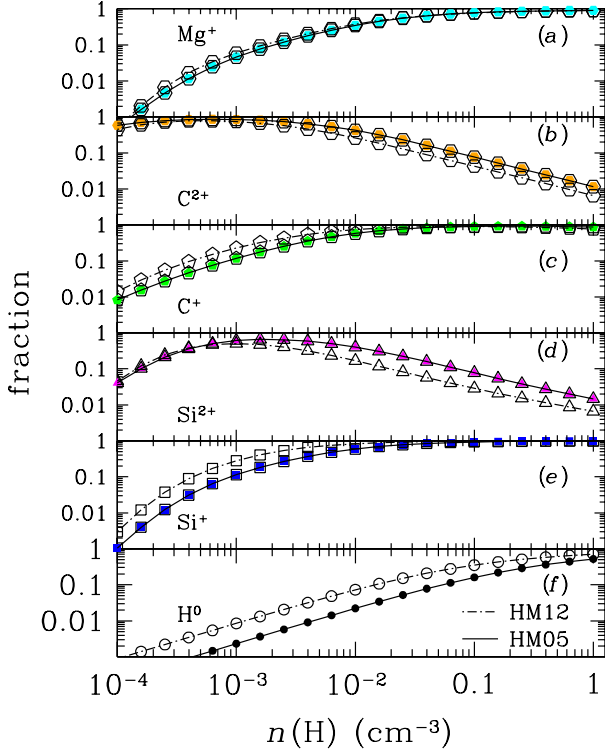


Figure 2. Expected fractions of different species as a function of gas density at $z = 0.2$ for the HM12 (a harder spectrum; open symbols with dash-dotted curves) and HM05 (a softer spectrum; close symbols with solid curves) ionizing spectra in Figure 1. The calculations are performed using the *Cloudy* software. The fraction of H^0 is found uniformly higher under HM12 than HM05 across the entire gas density range studied (panel *f*). At the same time, the fractions of C^{2+} and Si^{2+} are lower at $n(\text{H}) \gtrsim 10^{-3} \text{ cm}^{-3}$ under HM12 (panels *b* & *d*), while a reversed trend is seen under HM12 for C^+ and Si^+ at low densities, $n(\text{H}) \lesssim 10^{-2} \text{ cm}^{-3}$ (panels *c* & *e*) and Mg^+ displays very small changes (panel *a*) over the same gas density range. The differential corrections between hydrogen and other ions for different ionizing spectra naturally result in dramatically different estimates of gas metallicity for the same absorption systems (cf. Werk et al. 2014; Prochaska et al. 2017).

A common practice in CGM/IGM metallicity analyses is to (1) adopt the observed relative abundances in different ionization states, such as Si^+ and Si^{2+} , for constraining the ionization state of the gas, and (2) compare the relative abundances between H^0 and these heavy ions to infer a gas metallicity based on the expected ionization fraction corrections (e.g., Stocke et al. 2013; Lehner et al. 2013; Werk et al. 2014; Prochaska et al. 2017). However, because of the differential cross-section weighting in the photo-ionization rates of different species, it is expected from Figure 1 that different species would exhibit very different ionization fractions under different ionizing radiation fields (see also Crighton et al. 2015; Keeney et al. 2017).

To quantify such differences, we have computed the expected fractions in H^0 , Si^+ , Si^{2+} , C^+ , C^{2+} , and Mg^+ for different ionizing spectra. The results are presented in Figure 2. The calculations are performed using the *Cloudy* software for the HM12 (open symbols with dash-dotted curves) and HM05 (close symbols with solid curves) models presented in Figure 1. These calculations assume a plane-parallel geometry, a neutral hydrogen column density of $N(\text{HI}) = 16$, and a gas metallicity of 0.1 solar. Two distinct features are immediately clear in Figure 2. First of all, the fraction of H^0 is uniformly higher under HM12 than HM05 across the entire gas density range studied (panel *f*). This is understood as a combined result of lower J_ν at 1-3 Rydberg under the HM12 model and a monotonically-declining $\sigma(\text{H})$, with increasing photon energy (Figure 1). Secondly, this higher fraction of H^0 is accompanied by a lower fraction of C^{2+} and Si^{2+} at $n(\text{H}) \gtrsim 10^{-3} \text{ cm}^{-3}$ (panels *b* & *d*), while a reversed trend is seen for C^+ and Si^+ at low densities, $n(\text{H}) \lesssim 10^{-2} \text{ cm}^{-3}$ (panels *c* & *e*). Furthermore, the fraction of Mg^+ appears to be insensitive to the adopted ionizing spectrum (panel *a*). Figure 2 shows that adopting a different input ionizing spectrum can result in an order of magnitude difference in the inferred gas metallicity for the same observed relative abundances between HI and low-ionization species.

To further illustrate such systematic uncertainties in gas metallicity, we adopt galaxy #225_38 toward QSO J1220+3853 in the COS-Halos sample as an example (see Werk et al. 2013 for a summary). This galaxy is spectroscopically identified at $z = 0.27$ and $d = 154$ kpc from the sightline of the background QSO. A moderately strong $\text{Ly}\alpha$ absorber is identified at the redshift of the galaxy in the QSO spectrum. Werk et al. (2013) reported $\log N(\text{HI}) = 15.8 \pm 0.05$ based on observations of higher-order Lyman series lines, and placed constraints for associated low-ionization species at $\log N(\text{CII}) < 13.6$, $\log N(\text{CIII}) > 14.3$, $\log N(\text{SiII}) < 13.0$, and $\log N(\text{SiIII}) > 13.5$.

Werk et al. (2014) performed a photo-ionization analysis using the Haardt & Madau (2001; HM01) model¹ as the input ionizing spectrum, and reported a best-estimated gas metallicity of $[Z/\text{H}] = -0.6 \pm 0.2$. Recently, Prochaska et al. (2017) adopted the HM12 model and re-examined the ionization conditions of the COS-Halos sample. For the same $N(\text{HI})$ and column density constraints for low ions, these authors reported a best-estimated gas metallicity of $[Z/\text{H}] = +0.7 \pm 0.4$ for the CGM of this galaxy, a factor of 20 times higher than the earlier finding.

To better understand the origin of such discrepancy, we show in Figure 3 the predicted column densities of Si^+ (squares) and Si^{2+} (triangles) versus gas density under the HM12 (a harder spectrum; open symbols with dash-dotted curves) and HM05 (a softer spectrum; close symbols with solid curves) ionizing spectra for the COS-Halos galaxy

¹ The HM01 model is similar in shape to the HM05 spectrum but with a factor of 2–3 lower in amplitude near the Lyman edge.

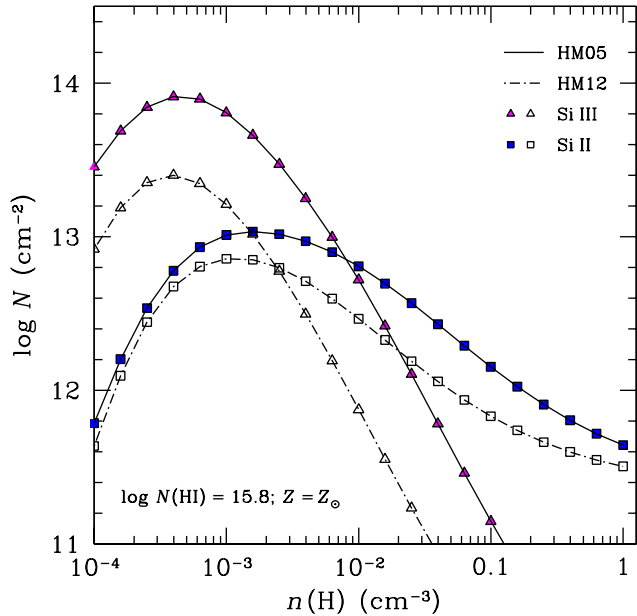


Figure 3. Predicted silicon ionic column densities as a function of gas density under the HM12 (a harder spectrum; open symbols with dash-dotted curves) and HM05 (a softer spectrum; close symbols with solid curves) ionizing spectra for the COS-Halos galaxy #225_38 at $z = 0.27$. The calculations are performed using the *Cloudy* software for $\log N(\text{HI}) = 15.8$ and solar metallicity. The predicted column densities will change proportionally with gas metallicity, but the overall trend remains. Under the HM12 ionizing radiation field, the abundance of Si III (triangles) is at least 0.5 dex smaller than expected from HM05. Consequently, for an observed $N(\text{SiIII})$, the required gas metallicity is higher under HM12 than under HM05.

#225_38 at $z = 0.27$. The calculations are performed using the *Cloudy* software for gas of $\log N(\text{HI}) = 15.8$ (appropriate for the COS-Halos example) and solar metallicity. A higher metallicity will lead to higher ionic column densities and vice versa, but the overall trend remains. The observed limits of $\log N(\text{SiIII}) \gtrsim 13.5$ and $\log N(\text{SiII}) < 13$ constrain the gas density in the $n(\text{H}) \lesssim 0.002 \text{ cm}^{-3}$ regime in both HM05 and HM12. Under the HM12 ionizing radiation field, however, a super-solar metallicity is required for the CGM of this COS-Halos galaxy in order to match the limit of $\log N(\text{SiIII}) > 13.5$, but this model would also violate the constraints placed by $N(\text{CII})$. In contrast, the observed limits of $N(\text{SiII})$, $N(\text{SiIII})$, $N(\text{CII})$, and $N(\text{CIII})$ can all be met for this absorber under HM05 for a gas metallicity of 40–60% solar.

4. DISCUSSION

The exercise presented in § 3 demonstrates that a harder UVB spectrum leads to a higher estimated gas metallicity for fixed ionic column densities. Therefore, such systematic uncertainties due to an uncertain ionizing radiation field must be included in the error budget for estimating metallicities of

ionized gas (see e.g., Crighton et al. 2015). Meanwhile, the expectation of different relative ionic ratios under different ionizing spectra from Figures 2 & 3 indicates that such uncertainties can be reduced if empirical diagnostics are available for discriminating between hard and soft ionizing spectra (see also Rauch et al. 1997).

Motivated by the reversed trend in the fractions of silicon ions when switching between HM12 (hard) and HM05 (soft) models in Figure 2, we first define the Si_{23} index according to the column density ratio between Si^+ and Si^{2+} , $Si_{23} \equiv \log N(\text{SiII})/N(\text{SiIII})$, and compare Si_{23} with column density ratios of additional ions. For this exercise, we utilize the same *Cloudy* models computed for the COS-Halos example in Figure 3, namely adopting the HM12 and HM05 spectra at $z = 0.27$ for absorbing gas of $\log N(\text{HI}) = 15.8$ and solar metallicity. We re-iterate that the overall trends are not sensitive to the adopted gas metallicity or $N(\text{HI})$ in the optically thin regime.

In Figure 4a, we compare Si_{23} with $C_{24} \equiv \log N(\text{CII})/N(\text{CIV})$ expected from the *Cloudy* models. Figure 4a shows that under HM12 the expected Si_{23} is 0.3 dex higher than predictions from HM05 for a fixed C_{24} . This can be explained based on the understanding that Si^{2+} is rapidly ionized to produce more Si^{3+} ions under a harder ionizing spectrum. Comparing Si_{23} and C_{24} bears the advantage that both are based on the same element but in different ionization states. Therefore, they are not subject to uncertainties in the intrinsic chemical enrichment pattern or differential dust depletions. However, additional caveats for C_{24} include its sensitivity to gas temperature (e.g., Haehnelt et al. 1996; Boksenberg & Sargent 2015) and the possibility that different ions may not be co-spatial. In principle, these can be addressed based on the observed absorption profiles in sufficiently high S/N and high spectral resolution spectra.

Alternatively, we compare Si_{23} with $\alpha_{22} \equiv \log N(\text{SiII})/N(\text{MgII})$ in Figure 4b. While α_{22} involves two different elements, both silicon and magnesium are α -elements with a comparable enrichment level (e.g., McWilliam 2016) and a similar degree of dust depletion (e.g., Savage & Sembach 1996; Jenkins 2009; De Cia et al. 2016). Therefore, we expect that uncertainties due to different chemical enrichment sources and differential dust depletion are at a minimum. Figure 4b shows that α_{22} is relatively insensitive to Si_{23} for the full gas density range considered here, namely $n(\text{H}) = 0.0001\text{--}1 \text{ cm}^{-3}$ shown in Figure 3. At the same time, α_{22} is sensitive to the spectral slope of the ionizing spectrum. The HM12 model predicts a factor of two more Si^+ relative to Mg^+ than the HM05 model. This is understood as Mg^+ being more ionized to higher ionization states under a harder ionizing spectrum.

In summary, we have shown that metallicity estimates of ionized gas require an accurate model of the ionization state of the gas which, in addition to gas density, depends on both the intensity and spectral slope of the ionizing radiation field. We have demonstrated that a harder UVB spectrum would result in a higher estimated gas metallicity for a given set of observed ionic column densities. Our initial effort in search

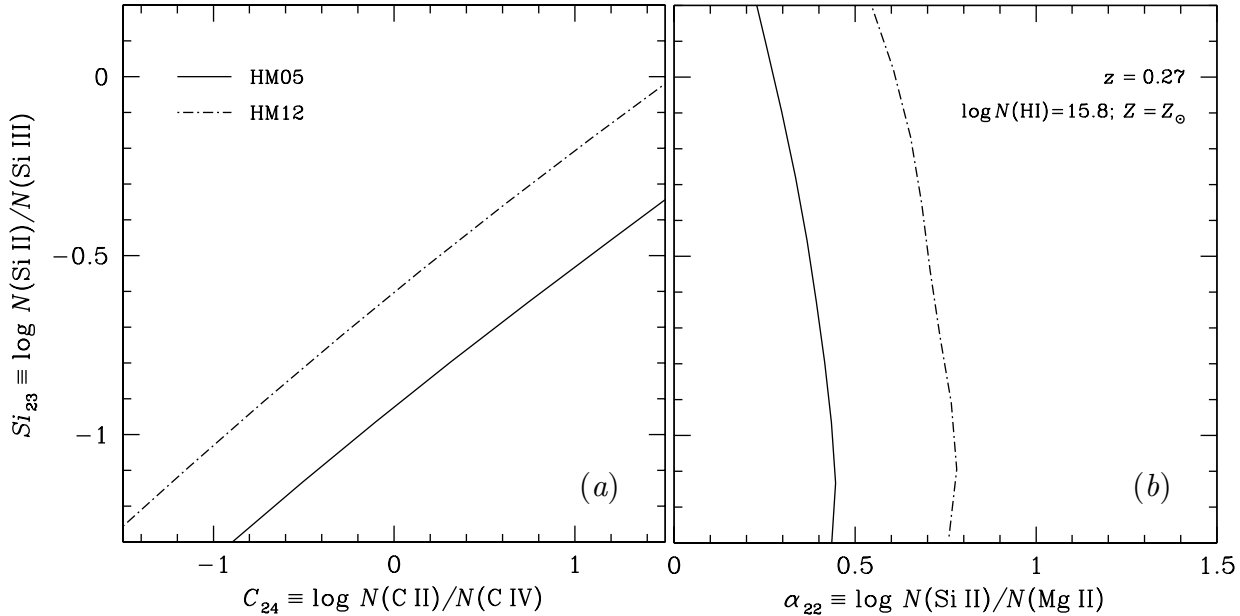


Figure 4. Empirical diagnostics for the spectral slope of the intrinsic ionizing spectrum. The expectation of different relative ionic ratios under different ionizing spectra offers a valuable tool for discriminating between hard and soft ionizing spectra. Adopting the same Cloudy models from Figure 3 and incorporating additional ionic ratios, Panel (a) shows that under HM12 the expected $N(\text{SiII})/N(\text{SiIII})$ ratio is 0.3 dex higher than predictions from HM05 for a fixed $N(\text{CII})/N(\text{CIV})$ ratio. In addition, the relative $N(\text{SiII})/N(\text{MgII})$ ratio is found to be insensitive to the gas density (or the $N(\text{SiII})/N(\text{SiIII})$ ratio), but depends sensitively on the spectral slope of the ionizing spectrum. The HM12 model predicts a factor of two more Si^+ relative to Mg^+ than the HM05 model. Combining Si_{23} with either C_{24} or α_{22} therefore places strong constraints for the underlying ionizing radiation field, and thereby reducing uncertainties in gas metallicity estimates.

of empirical diagnostics for the underlying ionization radiation field has yielded encouraging results. We find that by comparing the relative abundance ratio of Si^+ and Si^{2+} ions (Si_{23}) with either C^+/C^{3+} (C_{24}) or Si^+/Mg^+ (α_{22}), one can distinguish between hard and soft ionizing spectra and reduce the systematic uncertainties in the estimated gas metallicity. Ultimately, accurate estimates and associated uncertainties of CGM metallicity will require simultaneous modeling of both the gas metallicity and ionizing background. In the meantime, a broad spectral coverage to include prominent transitions from these ions is strongly encouraged for future CGM studies with a goal to constrain gas metallicity.

The authors thank Nick Gnedin for helpful comments on an initial draft. HWC acknowledges partial support from HST-GO-14145.01A. SDJ acknowledges support by NASA through a Hubble Fellowship grant HST-HF2-51375.001-A. FSZ is grateful for support from The Brinson Foundation and The Observatories of the Carnegie Institution for Science.

Software: Cloudy (Ferland et al. 2013), Starburst99 (Leitherer et al. 1999)

REFERENCES

- Aguirre, A. et al. 2001, *ApJ*, 561, 521
 , Balogh, M. L., Navarro, J. F., & Morris, S. L. 2000, *ApJ*, 540, 113
 Becker, G. D., Bolton, J. S., & Lidz, A. 2015, *PASA*, 32, 45
 Boksenberg, A. & Sargent, W. .L. W. 2015, *ApJS*, 218, 7
 Bordoloi, R. et al. 2011, *ApJ*, 743, 10
 Bordoloi, R. et al. 2014, *ApJ*, 796, 136
 Borthakur, S. et al. 2013, *ApJ*, 768, 18
 Chen, H.-W. et al. 1998, *ApJ*, 498, 77
 Chen, H.-W. et al. 2010, *ApJ*, 714, 1521
 Cool, R. J. et al. 2012, *ApJ*, 748, 10
 Crighton, N. H. M. et al. 2015, *MNRAS*, 446, 18
 De Cia, A. et al. 2016, *A&A*, 596, 97
 Faucher-Giguère, C.-A. et al. 2008, *ApJ*, 688, 85
 Ferland, G. J., Porter, R. L., van Hoof, P. A. M., et al. 2013, *RMxAA*, 49, 137
 Gunn, J. E. & Gott, III, J. R. 1972, *ApJ*, 176, 1
 Haardt, F., & Madau, P. 2001, in *Clusters of Galaxies and the High Redshift Universe Observed in X-rays*, ed. D. M. Neumann & J. T. V. Tran (Saclay:CEA), 64
 Haardt, F. & Madau, P. 2005, unpublished spectra in 2005 August update to Haardt & Madau (2001) and included in the photo-ionization code CLOUDY

- Haardt, F. & Madau, P. 2012, *ApJ*, 746, 125
- Haehnelt, M. G., Rauch, M., & Steinmetz, M. 1996, *MNRAS*, 283, 1055
- Huang, Y.-H. et al. 2016, *MNRAS*, 455, 1713
- Jenkins, E. B. 2009, *ApJ*, 700, 1299
- Johnson, S. D., Chen, H.-W., & Mulchaey, J. S. 2015, *MNRAS*, 449, 3263
- Kacprzak, G. et al. 2014, *ApJ*, 792, L12
- Keeney, B. A. et al. 2017, *ApJS*, 230, 6
- Kollmeier, J. A. et al. 2014, *ApJL*, 789, L3
- Kulkarni, V. P. et al., 2007, *ApJ*, 661, 88
- Lehner, N. et al. 2013, *ApJ*, 770, 138
- Leitherer, C., Schaerer, D., Goldader, J. D., et al. 1999, *ApJS*, 123, 3
- Liang, C. J. & Chen, H.-W. 2014, *MNRAS*, 445, 2061
- Lovegrove, E. & Simcoe, R. A. 2011, *ApJ*, 740, 30
- Madau, P. & Shull, J. M. 1996, *ApJ*, 457, 551
- McQuinn, M. 2016, *ARA&A*, 54, 313
- McWilliam, A. 2016, *PASA*, 33, 40
- Osterbrock, D. E., & Ferland, G. J. 2006, *Astrophysics of Gaseous Nebulae and Active Galactic Nuclei* (2nd edn.; Sausalito: University Science Books), 18
- Péroux, C. et al., 2003, *MNRAS*, 345, 480
- Péroux, C. et al., 2016, *MNRAS*, 457, 903
- Prochaska et al. 2017, *ApJ*, 837, 169
- Rauch, M., Haehnelt, M. G., & Steinmetz, M. 1997, *ApJ*, 481, 601
- Rudie, G. C. et al. 2012, *ApJ*, 750, 67
- Savage, B. D. & Sembach, K. R. 1996, *ARA&A*, 34, 279
- Scannapieco, E., Ferrara, A., & Madau, P. 2002, *ApJ*, 574, 590
- Scott, J. E. et al. 2004, *ApJ*, 615, 135
- Shen, S. et al. 2013, *ApJ*, 765, 89
- Shull, J. M. et al. 2015, *ApJ*, 811, 3
- Somerville, R. S. & Davé, R. 2015, *ARA&A*, 53, 51
- Steidel, C. C. et al. 2010, *ApJ*, 717, 289
- Stocke, J. T., et al. 2013, *ApJ*, 763, 148
- Tumlinson, J. et al. 2011, *Science*, 334, 948
- Verner, D. A. et al. 1996, *ApJ*, 465, 487
- Werk, J. et al. 2013, *ApJ*, 204, 17
- Werk, J. et al. 2014, *ApJ*, 792, 8